

Power Switch Open-Circuit Fault Detection in an Interleaved DC/DC Buck Converter for Electrolyzer Applications by Using Curvilinear Component Analysis

G.Cirincione

LTI-University of Picardie Jules Verne,
80000, Amiens, France
Amiens, Italy
giansalvo.cirincione@u-picardie.fr

M.Cirincione

University of the South Pacific
Suva, Fiji
maurizio.cirincione@usp.ac.fj

D.Guilbert*

Université de Lorraine, IUT de
Longwy, GREEN
France
damien.guilbert@univ-lorraine.fr

A.Mohammadi

University of the South Pacific
Suva, Fiji
ali.mohammadi@usp.ac.fj

V. Randazzo

Politecnico di Torino, Italy
vincenzo.randazzo@polito.it

Abstract— Nowadays, the use of electrolyzers to cleanly and efficiently generate hydrogen from renewable energy sources is an attractive solution. Like fuel cell systems, DC/DC converters are needed to interface the DC bus with the electrolyzer. Classic buck converters are generally used for this purpose. However, these topologies must meet several requirements from output current ripple reduction and availability in case of electrical failures point of view. Hence, an interleaved DC/DC buck converter has been chosen as a viable solution in order to meet these requirements. With the aim of improving the availability and reliability of the DC/DC converter, the development of a power switch fault detection method is mandatory. This paper proposes a novel power switch fault detection method based on a non-linear dimensionality reduction technique, implemented by means of a neural network. Experimental tests are carried out for demonstrating the performance of the proposed strategy to accurately detect the faulty leg.

Keywords—electrolyzer, dc-dc converter, power switch fault diagnosis, reliability, curvilinear component analysis.

I. INTRODUCTION

Among the different existing processes to produce hydrogen, water electrolysis appears as a promising and attractive option if renewable energy sources (RES) are used [1]. Electrolysis is a process which uses electrical energy to split water into hydrogen and oxygen and is carried out by means of an electrolyzer (EL). Due to the low DC voltage required at the input of the EL, a DC/DC converter is needed, typically a DC/DC buck converter [2]. However, this topology presents several drawbacks particularly in terms of reliability in case of power switch failures, because they are ranked as the most fragile components. Indeed, over 30% of reported failures in DC/DC converters are due to them [3]. In this research work, an Interleaved Buck DC/DC converter (IBC) has been selected. Indeed, this topology presents several advantages, particularly from energy efficiency, reduced output current ripple, and availability in case of power switch failures point of view. Therefore, this topology is particularly suitable for EL applications; where the availability of the DC/DC converter is required [4].

However, in order to guarantee a high level of reliability regarding keeping its function, the development of a power

switch fault detection method and Fault-Tolerant Control (FTC) is mandatory.

So far, few papers [5]-[11] have been reported in the literature regarding power switch failure detection in interleaved DC/DC converter topologies. Ribeiro et al. [5] have developed an open-circuit fault (OCF) detection method for a 3-leg interleaved DC/DC boost converter, where the OCF detection method is based on the input current derivative. However, the paper does not present any energy management after fault detection in spite of additional electrical stresses on healthy components [12]. By comparison, Poon et al. [6] have proposed a power switch fault detection method, both OCF and short-circuit fault (SCF), for a 6-leg interleaved DC/DC boost converter, where the detection method is based on a model-based estimator approach. Bento and Cardoso [7] have developed an OCF detection method based on the input current for a 3-leg interleaved DC/DC boost converter. Once the OCF is detected, phase and frequency of each PWM signal are adjusted according to the location of the failure. An OCF can be detected in 0.53ms. Long time detection is explained by the use of a dSPACE prototyping system and the low switching frequency of the converter (i.e. 1 kHz). Pazouki et al. [8] have developed a SCF detection method based on the input current derivative monitoring for a 3-leg interleaved DC/DC boost converter. SCFs can be detected in 50 μ s. Shahbazi et al. [9] have described an OCF detection method for a 3-leg interleaved boost converter: this method is cost-attractive since it only needs one current sensor (input current). Finally, Yahyaoui et al. [10] have developed a SCF detection method based on drain-to-source voltage monitoring for a 6-leg interleaved DC/DC boost converter to be used in fuel cell electric vehicle (FCEV) applications: because of the number of legs, however, the proposed fault detection method requires six additional sensors in order to detect accurately the faulty leg; which makes it unattractive for FCEVs. In [11], the authors have proposed a SCF management. The post-failure operation consists in adjusting the phase shift between the remaining healthy legs and integrating an additional pattern which substitutes the faulty leg.

Based on the existing literature of this research topic of emerging interest [5]-[11], the purpose of this paper is to develop an original non-invasive fault detection method for OCF based on a non-linear dimensionality reduction

technique, implemented by means of a neural network and avoiding the use of additional sensors.

This work is divided into three sections. After the introduction, providing the current state-of-the-art and the motivations, section 2 presents the experimental test bench. Finally, in section 3, the developed fault detection method based on a non-linear dimensionality reduction technique is introduced. Besides, results are provided to validate the effectiveness of the developed fault detection method to accurately detect the faulty leg.

II. EXPERIMENTAL TEST BENCH DESCRIPTION

In order to carry out a thorough investigation of the undesirable effects as a result of an OCF, experimental tests have been performed on the test bench shown in Fig. 1. This bench is composed of a DC power supply, a 3-leg IBC, a Proton Exchange Membrane (PEM) EL, metal hydride hydrogen tanks, a measurement board (i.e. leg currents and DC bus voltage), a microcontroller for control purpose, driver boards to control the power switches and finally a PC. The EL is provided in de-ionized water from a tank under pressure.

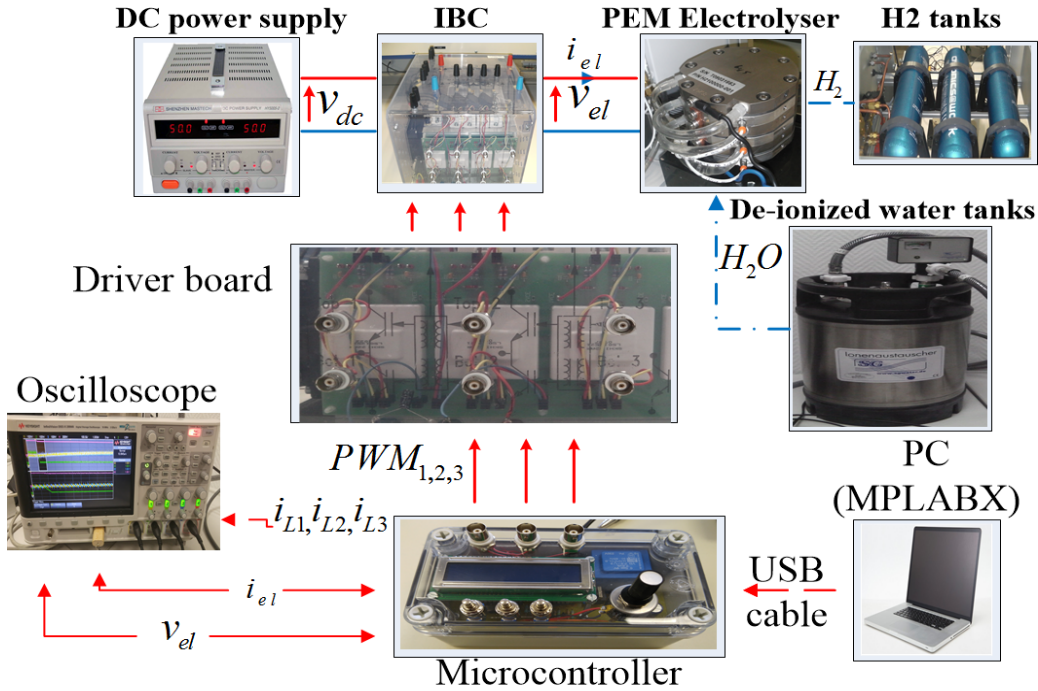


Fig.1. Experimental test bench.

OCFs have been simulated with the help of push-buttons linked to the microcontroller. Each push-button is assigned to a specific pin number and is combined with a PWM gate control signal. On the one hand, when the push-button is not pressed, the PWM gate control signal is sent to driver boards. On the other hand, if the push-button is pressed, the PWM gate control signal can be forced to “0” with resulting generation of an OCF. The system specifications of the experimental test bench are summarized in Table I.

TABLE I. SYSTEM SPECIFICATIONS

Parameters	Values
EL Rated power, P_{el}	400 W
EL rated current, I_{el}	50 A
EL current ripple, ΔI_{FC}	1 A
EL voltage range (ohmic region), V_{FC}	7.5-8 V
Inductor, L	400 μ H
Input DC bus voltage, V_{DC}	50V
Switching frequency, F_s	20 kHz
Duty cycle range, D	0.23-0.26

III. POWER SWITCH FAULT DETECTION METHOD

In order to automatically detect a fault in any of the three legs of the IBC, a nonlinear dimensionality reduction technique, implemented by means of a Curvilinear Component Analysis (CCA) neural network [13], is proposed here, which allows the use of redundant features for diagnostic. An OCF on the second leg has been simulated (highlighted in red) and the results are given in Fig. 2. Since the output current (i.e. EL current) is used for control purposes, it has been analyzed by the CCA to detect the failure. As it has been emphasized in the Introduction section, no additional sensors for diagnostic purposes have been used because they increase cost and complexity while downgrading the overall reliability of the system.

A. Data Preprocessing

For feature detection and extraction, it has been chosen to use only time information to have a fast response. In particular, 15 features have been extracted from the output current by using a mobile time window of ten-time instants, which has yielded the best results. Indeed, these fifteen temporal features have been chosen for representing as better as possible the time behavior. The neural network for projection will eventually reveal the true dimensionality of data and the corresponding nonlinear projection.

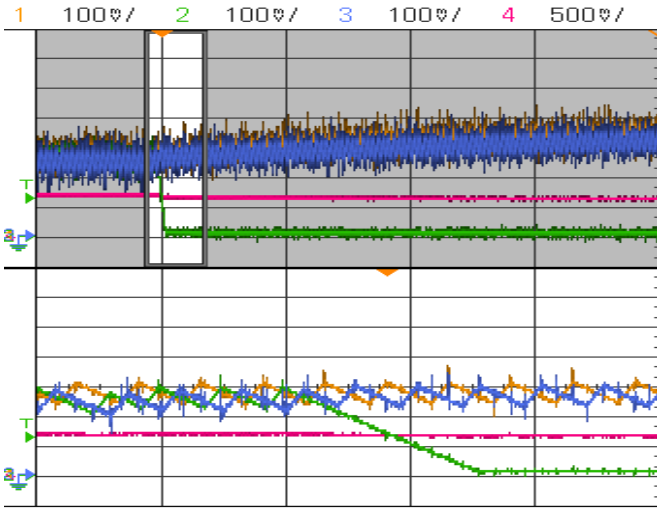


Fig. 2: Leg and output currents in transient state after fault-occurrence, channel 1 : leg 1 current (1A/div), channel 2 : leg 2 current (1A/div), channel 3 : leg 3 current (1A/div), channel 4: EL current (5A/div).

The adopted time features have been:

- | | |
|----------------------------|-------------------------------|
| 1. Mean | 9. Crest factor |
| 2. Maximum value | 10. Latitude factor |
| 3. Root mean square (RMS) | 11. Impulse factor |
| 4. Square root mean (SRM) | 12. Skewness |
| 5. Standard deviation | 13. Kurtosis |
| 6. Variance | 14. Normalized central moment |
| 7. Shape factor (with SRM) | 15. Normalized central moment |
| 8. Shape factor (with SRM) | |

Indeed, these fifteen temporal features have been chosen for representing as better as possible the time behavior. The neural network for projection will eventually reveal the true dimensionality of data and the corresponding nonlinear projection. The 15-features dataset has then been normalized by using the statistical scaling (mean zero, variance one).

B. Curvilinear Component Analysis

In order to analyze the onset of the fault from a topological point of view, a non-linear dimensionality reduction is needed for the exploitation of a possibly large number of temporal features. One of the most important non-linear tools for dimensionality reduction is the Curvilinear Component Analysis (CCA, [13]) which is a non-convex technique based on weighted distances.

It derives from the Sammon mapping [14] but improves it because of its properties of unfolding data and extrapolation. CCA is a self-organizing neural network (see Fig.3), which performs the quantization of a data training set (input space, say X) for estimating the corresponding non-linear projection into a lower dimensional space (latent space, say Y). Two weights are attached to each neuron.

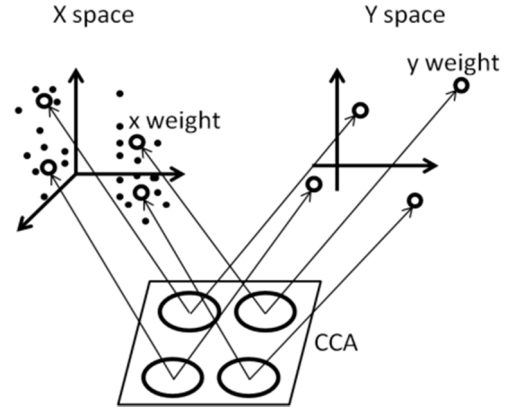


Fig. 3: The CCA neural network and its two weight layers.

For each pair of different weight vectors in the X space (data space), an in-between point distance D_{ij} , is calculated as:

$$D_{ij} = \|x_i - x_j\| \quad (1)$$

The objective is to constraint the distance L_{ij} of the associated Y-weights in the latent space, computed as:

$$L_{ij} = \|y_i - y_j\| \quad (2)$$

Equation (2) must be equal to D_{ij} . Obviously, this is possible only if all input data lay on a linear manifold. To address this problem, CCA defines a metric function F_λ , which penalizes the long distances, but preserves local topology, by using a user-dependent parameter λ . In its simplest form, it is given by:

$$F_\lambda(L_{ij}) = \begin{cases} 0 & \lambda < L_{ij} \\ 1 & \lambda \geq L_{ij} \end{cases} \quad (3)$$

That is a step function for constraining only the under threshold between-point distances L_{ij} . Defining y_j as the weight of the j-th projecting neuron, the stochastic updating formula is given by:

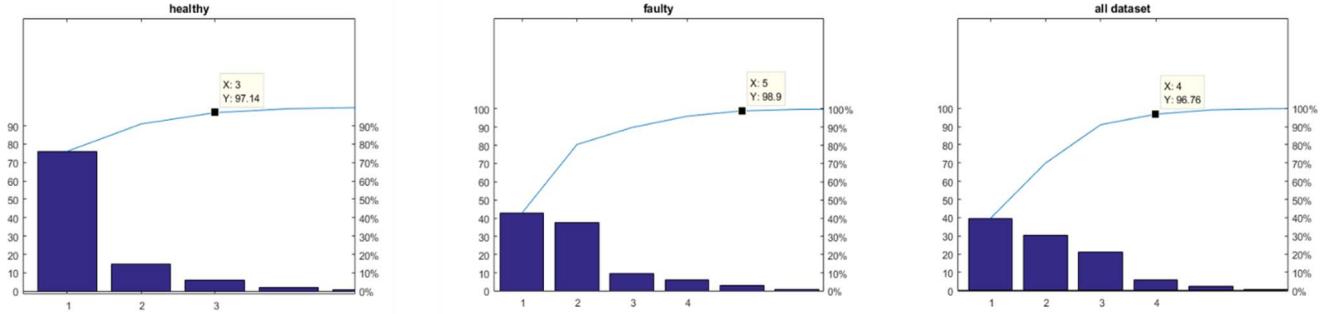
$$y_i(t+1) = y_i(t) + \alpha(D_{ij} - L_{ij})F_\lambda(L_{ij}) \frac{y_j(t) - y_i(t)}{L_{ij}} \quad (4)$$

where α is the learning rate.

Associated to CCA is the $dy-dx$ diagram; which is the plot of the distances of samples in the latent space (dy) versus the distances of corresponding samples in the data space (dx). In this scenario, it acts as a tool for the detection and analysis of nonlinearities. Generally, the more the deviation of data cloud with respect to the bisector, the more nonlinear the manifold is.

C. Analysis of the Data Manifold

The manifolds in which lay data for either the healthy or the faulty state are analyzed in order to determine the best possible classification. At this aim, firstly, a linear approach (Pareto analysis) is proposed for having an idea of their



intrinsic dimensionality. Then, CCA is used to refine this study.

Fig. 4 shows the Pareto (Principal Component Analysis) diagrams for the healthy (left), faulty (middle) and both (right) states, respectively. The healthy manifold is basically two dimensional (the other three principal components are probably due to noise). Notice the difference between the first and the second components. Instead, the faulty manifold is four dimensional. However, the two first principal components have similar values. Interestingly, also the global state is four dimensional, but the difference between the first and the second components is as high as the healthy case. It

Fig. 4 Pareto diagrams for the three datasets: only-healthy (left), only-faulty (middle), global (right)

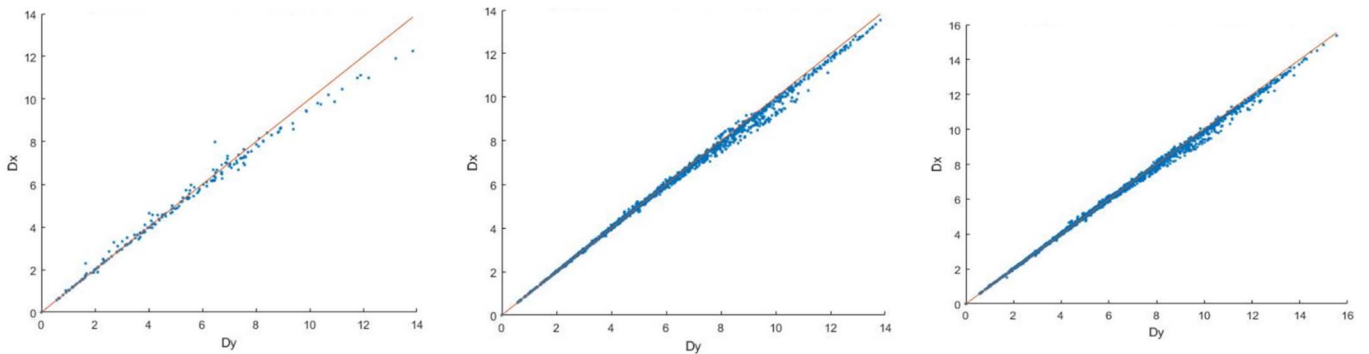


Fig. 5 $dydx$ CCA diagrams for the three datasets: only-healthy (left), only-faulty (middle), global (right). The values of the CCA parameters are: projection dim = 2, $\lambda = 60$, $\alpha = 0.5$, epochs = 100 (only-healthy), projection dim = 4, $\lambda = 10$, $\alpha = 0.5$, epochs = 100 (only-faulty), projection dim = 4, $\lambda = 10$, $\alpha = 0.5$, epochs = 10 (global)

suggests that the healthy state does not contribute much to the global manifold. This conclusion is confirmed by the analysis of the principal angles between the healthy and faulty manifolds. Indeed, they are given by 1.98° and 8.08° (assuming manifolds are flats, as will be basically confirmed by the next CCA analysis). The first principal angle is near zero, because of noise. Also, the second angle is small. It can be argued that the two *flats* have one-dimensional intersection and are slightly tilted. This justifies the reduced impact of the first two (very different) principal components of the healthy manifold in the global (see Fig. 4 right) Pareto diagram.

The non-linear analysis, by using the CCA $dydx$ diagrams confirms that, in a first approximation, the manifolds are *flats*.

Fig. 5 left corresponds to the 2-D projection of the healthy manifold. For small and medium distances data are well around the bisector. For larger distances, it bends under the bisector. It means that the healthy manifold is quasi-linear (the manifold is slightly folded). Fig 5 middle represents the 4-D projection of the faulty dataset. It is basically a four-dimensional *flat* with a slight folding. This inspection is

obviously confirmed in Fig. 5 right.

D. Classification

As a result of the previous analysis, it can be stated that, w.r.t. the projection space, a four dimensional manifold is the best suited to represent the input data while preserving its topology. This is confirmed by Figs. 6 and 7. Fig. 6 shows the 2-D projection of both the healthy (blue dots) and faulty (red dots) datasets. As expected from its Pareto diagram, a 2-D manifold is only sufficient to correctly represented the healthy state. On the contrary, even if the two datasets are

clearly separated, the faulty dataset is wrongly represented in a such low dimension space. The different red branches are not related to different faults but are, indeed, artifacts induced from the projection to the wrong dimension.

Fig. 7 shows the 3-D plot of the four dimensional projection of both the healthy (black dots) and faulty (red dots) datasets. The figure confirms what demonstrated in the previous subsection. Indeed, in a four dimensional space, both the datasets are properly represented, and no artifacts appear.

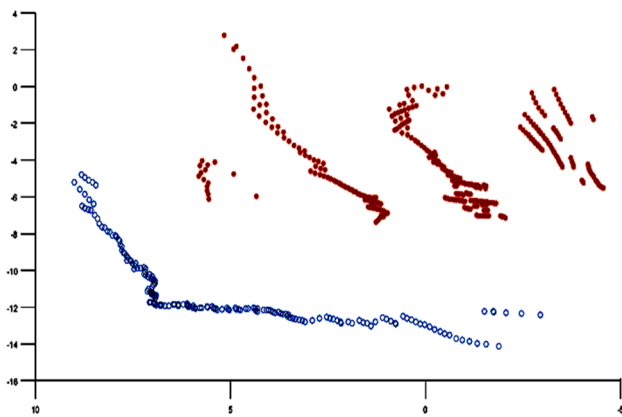


Fig. 6: 2-D scatter plot of the two dimensional projected datasets: healthy (blue dots) and faulty (red dots).

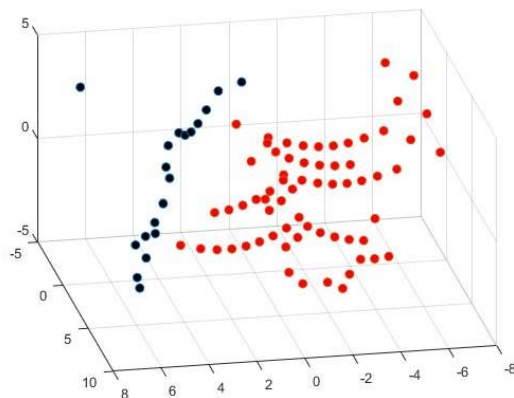


Fig. 7: 3-D scatter plot of the four dimensional projected datasets: healthy (black dots) and faulty (red dots).

IV. CONCLUSIONS

The main purpose of this work is to propose a novel power switch OCF detection method based on a non-linear dimensionality reduction technique, implemented by means of a neural network. The proposed OCF has been validated by using experimental results. Indeed, features of healthy and faulty operating mode have been extracted from the experimental data. Hence, based on fault signature, an OCF can be accurately identified and detected.

In summary, those preliminary results could be useful to develop short-circuit failures detection algorithm based on curvilinear component analysis.

I. REFERENCES

- [1] U.S. Department of Energy, Fuel Cell Technologies Office: 2016 Annual Merit Review Proceedings. Available online: https://www.hydrogen.energy.gov/annual_review16_proceedings.htm
- [2] T. Zhou, B. François, M. El Hadi Lebbal, S. Lecoeuche, "Real-Time Emulation of a Hydrogen-Production Process for Assessment of an Active Wind-Energy Conversion System", *IEEE Transactions on Industrial Electronics*, vol. 56, no. 3, pp. 737-746, 2009.3]
- [3] S. Yang, A. Bryant, P. Mawby, D. Xiang, R. Li, and P. Tavner, "An industry-based survey of reliability in power electronic converters", *IEEE Trans. Ind. Appl.*, vol. 47, no. 3, pp. 1441-1451, 2011.
- [4] D. Guilbert, S.M. Collura, A. Scipioni, « DC/DC converter topologies for electrolyzers: State-of-the-art and remaining key issues», *International Journal of Hydrogen Energy*, vol. 42, iss. 38, p. 23966-23985, 2017.
- [5] E. Ribeiro, A.J. Marques Cardoso, C. Boccaletti, "Open-Circuit Fault Diagnosis in Interleaved DC-DC Converters", *IEEE Transactions on Power Electronics*, Vol. 29, No. 6, pp. 3091-3102, 2014.
- [6] J. Poon, I.C. Konstantakopoulos, C. Spanos, S.R. Sanders, "Real-time model-based fault diagnosis for switching power converters", in: *Proceedings of IEEE Applied Power Electronics Conference and Exposition*, pp. 358-364, 2015.
- [7] F. Bento and A. J. M. Cardoso, "Open-circuit fault diagnosis in interleaved DC-DC boost converters and reconfiguration strategy," 2017 IEEE 11th International Symposium on Diagnostics for Electrical Machines, Power Electronics and Drives (SDEMPED), Tinos, pp. 394-400, 2017.
- [8] E. Pazouki, J. A. De Abreu-Garcia and Y. Sozer, "Short circuit fault diagnosis for interleaved DC-DC converter using DC-link current emulator," 2017 IEEE Applied Power Electronics Conference and Exposition (APEC), Tampa, FL, pp. 230-236, 2017.
- [9] M. Shahbazi, M. Reza Zolghadri, S. Ouni, "Fast and simple open-circuit fault detection method for interleaved DC-DC converters", in: *Proceedings of IEEE Power Electronics and Drive Systems Technologies Conference*, pp. 440-445, 2016.
- [10] R. Yahyaoui, A. De Bernardinis, A. Gaillard, D. Hissel, "Switch short-circuit fault detection algorithm based on drain-to-source voltage monitoring for a fault-tolerant DC/DC converter", in: *Proceedings of 42nd Annual Conference of the IEEE Industrial Electronics Society (IECON 2016)*, pp. 1-7, 2016.
- [11] R. Yahyaoui, A. Gaillard, A. De Bernardinis and D. Hissel, "Signal Processing-Based Switch Fault Detection Methods for Multi-Phase Interleaved Boost Converter," 2017 IEEE Vehicle Power and Propulsion Conference (VPPC), Belfort, pp. 1-6, 2017.
- [12] D. Guilbert, A. Gaillard, A. Mohammadi, A. N'Diaye, A. Djerdir, Investigation of the interactions between proton exchange membrane fuel cell and interleaved DC/DC boost converter in case of power switch faults, *International Journal of Hydrogen Energy*, vol. 40, no. 1, pp. 519-537, 2015.
- [13] P. Demartines and J. Héroult, "Curvilinear Component Analysis: A Self-Organizing Neural Network for Nonlinear Mapping of Data Sets", *IEEE Transaction on Neural Networks*, vol. 8, no. 1, pp. 148-154, 1997.
- [14] L. Van der Maaten, E. Postma and H. Van der Herik, *Dimensionality Reduction: a Comparative Review*, TiCC TR 2009-005, Delft University of Technology, 2009.